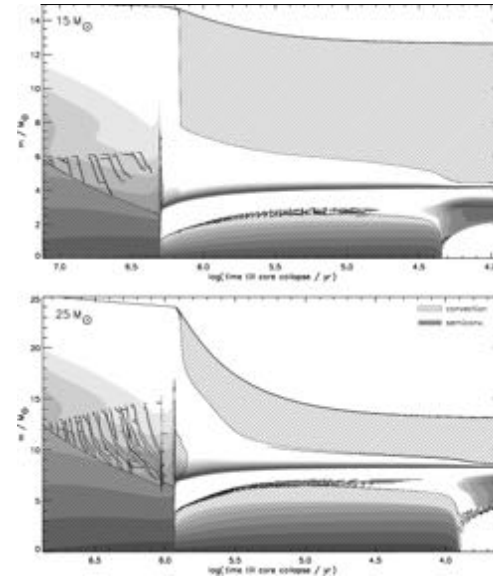


# Lecture 8

## Complications: Overshoot Mixing, Semiconvection, Mass Loss, and Rotation



The four greatest uncertainties in modeling stars, especially the presupernova evolution of massive stars are:

- Convection and convective boundaries (undershoot, overshoot, semiconvection, late stages)
- The effects of rotation and magnetic torques
- Mass loss (and its dependence on metallicity)
- Binary mass exchange

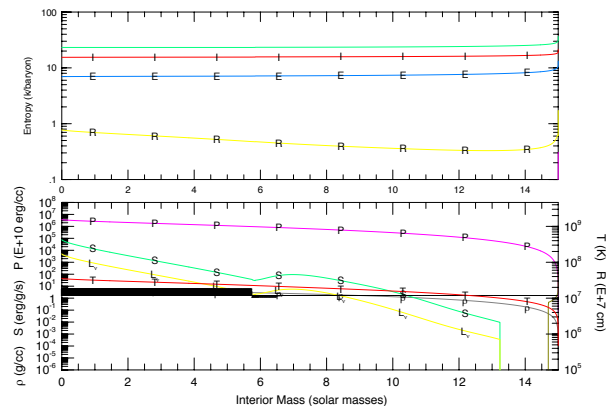
### Convective Overshoot (and Undershoot) Mixing

Initially the entropy is nearly flat in a zero age main sequence star so just where convection stops is a bit ambiguous. As burning proceeds and the entropy decreases in the center, the convective extent becomes more precisely defined. Still one expects some “fuzziness” in the boundary. Convective plumes should not stop at a precise entropy. Multi-D Calculations of entire burning stages are not feasible except perhaps in the very late stages ( $\tau_{nuc} \gg \tau_{conv}$ )

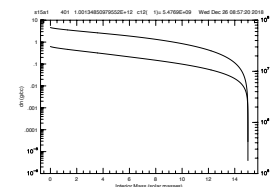
A widely adopted prescription is to continue arbitrarily the convective mixing beyond its mathematical boundary by some fraction,  $a$ , of the pressure scale height. Maeder uses 20%. Stothers and Chin (ApJ, 381, L67), based on the width of the main sequence, argue that it is less than about 20%. Doom, Chiosi, and many European groups once used larger values. Woosley and Heger use much less. Nomoto et al use none.

This is an area where multi-dimensional simulation has made some progress.

s15a1 594 9.79732031569851E+12 o16( 1)= 5.0000E+10 Wed Dec 26 08:45:12 2018  
R = 3.1275E+11 T\_eff = 3.2155E+04 L = 7.4495E+37 Iter = 5  
Dc = 6.8319E+00 Tc = 3.5202E+07 Ln = 5.2356E+36 Jm = 4375 Etot = -1.199E+50



Initially the entropy in a main sequence star is almost constant – 15 solar mass model at hydrogen ignition



Some references:

DeMarque et al, *ApJ*, **426**, 165, (1994) – modeling main sequence widths in clusters suggests  $\alpha = 0.23$

Woo and Demarque, *AJ*, **122**, 1602 (2001) – empirically for low mass stars, overshoot is < 15% of the core radius. Core radius a better discriminant than pressure scale height.

Brumme, Clune, and Toomre, *ApJ*, **570**, 825, (2002) – numerical 3D simulations. Overshoot may go a significant fraction of a pressure scale height, but does not quickly establish an adiabatic gradient in the region.

Meakin and Arnett, *ApJ*, **667**, 448 (2007) – treats overshoot mixing as an entrainment process sensitive to the Richardson number

Differential rotation complicates things and may have some of the same effects as overshoot.

## Convective Overshoot

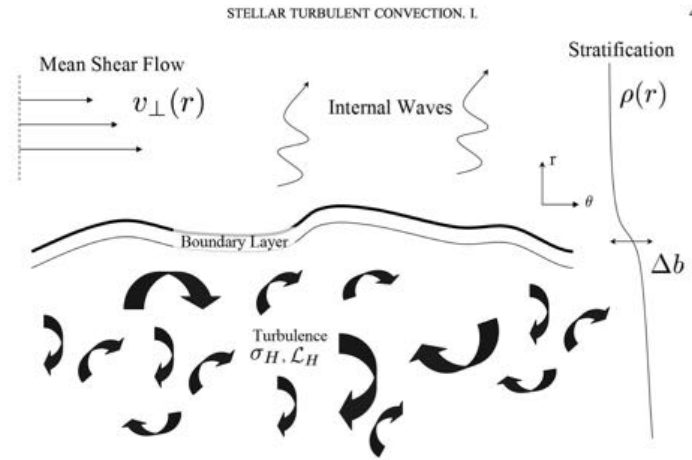


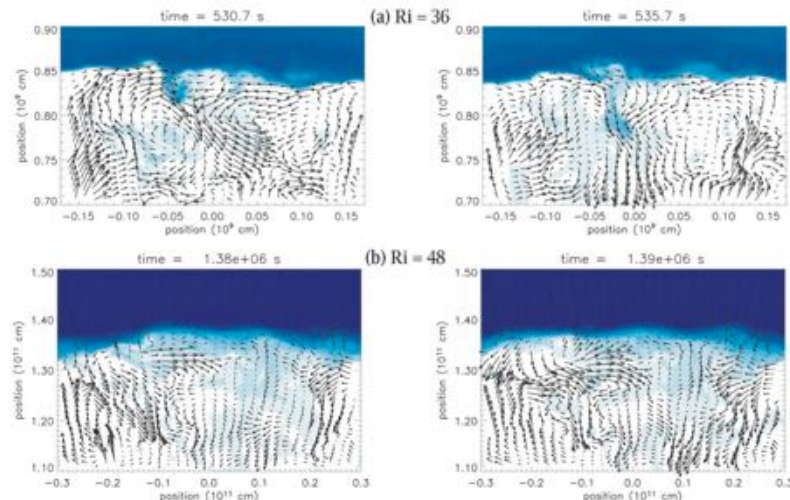
FIG. 1.—Diagram illustrating the salient features of the density and velocity field for the turbulent entrainment problem. Three layers are present: a turbulent convection zone is separated from an overlying stably stratified region by a boundary layer of thickness  $\delta$  and buoyancy jump  $\Delta b \sim N^2 \delta$ . The turbulence near the interface is characterized by integral scale and rms velocity  $L_H$  and  $\sigma_H$ , respectively. The stably stratified layer with buoyancy frequency  $N(r)$  propagates internal waves that are excited by the adjacent turbulence. A shear velocity field  $v_\perp(r)$ , associated with differential rotation, may also be present. After Strang & Fernando (2001).

Meakin and Arnett (*ApJ*, 667, 448, (2007))  
see also Arnett and Meakin (*ApJ*, 733, 78. (2013))

No. 1, 2007

STELLAR TURBULENT CONVECTION. I

467



Entrainment given by the Richardson number

$Ri = \frac{\Delta b L}{\sigma^2}$  where  $\Delta b$  is the change in buoyancy,  $L$ , the length scale and  $\sigma^2$  the turbulent velocity dispersion adjacent to the interface.

Meakin and Arnett (2007) – see class website

$$Ri = \frac{\Delta b L}{\sigma^2} \quad b(r) = -g \int_{r_1}^r \left( \frac{\partial \ln \rho}{\partial r} - \frac{\partial \ln \rho}{\partial r} \Big|_s \right) dr$$

$\sigma$  = turbulent velocity dispersion

$L$  = characteristic length scale for the turbulence

$b(r)$  = buoyancy - change in gravitational potential across boundary

$$\dot{M}_E = \frac{\partial M}{\partial r} u_E = (4\pi r_i^2 \rho_i) \sigma f_A 10^{(-n \log Ri)}$$

$f_A$  is the turbulent mixing efficiency < 1,  $1 < n < 1.75$ ,

and  $\dot{M}_E$  is the growth rate due to entrainment

Large  $Ri$  corresponds to stability – i.e., large buoyancy change and small velocity dispersion.  $u_E$  is the entrainment speed

Overshoot mixing is important for

- Setting the size of the cores, He cores during H burning, CO cores in helium burning. These greatly affect the later evolution of massive stars
- Altering the luminosity and lifetime on the main sequence
- Allowing interpenetration of hydrogen and helium in the thin helium shell flashes in AGB stars
- Mixing in the sun at the tachyocline
- Dredge up of H in classical nova outbursts
- Decrease in critical main sequence mass for C ignition
- Primary nitrogen production and more ...

## Semiconvection

A historical split in the way convection is treated in stellar evolution codes comes about because the adiabatic condition can be written two ways – one based on the temperature gradient, the other on the density gradient.

From the first law of thermodynamics - Non-degenerate gas (Clayton 118ff):

$$dQ = TdS = dU + PdV = 0 \text{ for an adiabatic process}$$

Setting this to zero can be used to eliminate T for  $\rho$  from the equation that contains P.

$$= \left( \frac{\partial U}{\partial T} \right)_V dT + \left( \frac{\partial U}{\partial V} \right)_T dV + PdV \quad V \equiv \frac{1}{\rho}$$

$$U = aT^4V + \frac{3}{2} \frac{N_A}{\mu} kT \quad P = \frac{1}{3} aT^4 + \frac{N_A}{\mu V} kT$$

Ignoring  $\mu$ -dependence:

$$\Gamma_1 = \frac{32 - 24\beta - 3\beta^2}{24 - 21\beta}$$

$$\Gamma_2 = \frac{32 - 24\beta - 3\beta^2}{24 - 18\beta - 3\beta^2} = 4/3 \text{ to } 5/3$$

$$dS = 0 \Rightarrow \begin{cases} \frac{dP}{P} - \Gamma_1 \frac{d\rho}{\rho} = 0, & \text{Ledoux} \\ \frac{dP}{P} + \frac{\Gamma_2}{1 - \Gamma_2} \frac{dT}{T} = 0, & \text{Schwarzschild} \end{cases}$$

The Schwarzschild criterion is most frequently found in textbooks:

$$\frac{dP}{P} + \frac{\Gamma_2}{1 - \Gamma_2} \frac{dT}{T} = 0 \Rightarrow \frac{1 - \Gamma_2}{\Gamma_2} \frac{dP}{P} + \frac{dT}{T} = 0$$

$$\left( \frac{dT}{dr} \right)_{rad} > \left( \frac{dT}{dr} \right)_{ad} = \left( 1 - \frac{1}{\Gamma_2} \right) \frac{T}{P} \frac{dP}{dr}$$

implies convection (Clayton 3-276)

$$-\frac{3}{4ac} \frac{\kappa \rho}{T^3} \frac{L(r)}{4\pi r^2} > \left( 1 - \frac{1}{\Gamma_2} \right) \frac{T}{P} \frac{dP}{dr} \quad \frac{dP}{dr} = -\frac{GM(r)\rho}{r^2}$$

$$\Rightarrow L_{crit} = \frac{16\pi acG}{3\kappa} \left( 1 - \frac{1}{\Gamma_2} \right) \frac{T^4}{P} M(r)$$

$$= \text{for ideal gas } 1.22 \times 10^{-18} \frac{\mu T^3}{\kappa \rho} M(r) \text{ erg/s}$$

$$\left. \right\} P = \frac{\rho N_A k T}{\mu}$$

But, in fact, the criterion for convection,  $dS > 0$ , can be written as either  $A > 0$  or  $B > 0$  where:

$$A = \frac{1}{\Gamma_1 P} \frac{dP}{dr} - \frac{1}{\rho} \frac{d\rho}{dr} \quad \text{density criterion} \quad \text{LeDoux}$$

nb. each term is negative because of the derivative

$$B = \frac{\Gamma_2 - 1}{\Gamma_2} \frac{1}{P} \frac{dP}{dr} - \frac{1}{T} \frac{dT}{dr} \quad \text{temperature criterion} \quad \text{Schwarzschild}$$

It can be shown for a mixture of ideal gas and radiation with variable composition that for  $\nabla_{rad} \equiv \frac{d \ln T}{d \ln P}$   $\nabla_L =$  threshold for Ledoux convection

$$\nabla_L = \nabla_s + \frac{\beta}{4 - 3\beta} \nabla_\mu \quad (\text{Langer et al 1983, 1985; Sakashita and Hayashi 1961; Kippenhan and Weigert - textbook - 6.12})$$

$$\text{where } \nabla_\mu = \frac{d \ln \mu}{d \ln P} \quad \nabla_s = \left( \frac{d \ln T}{d \ln P} \right)_{ad} \quad \nabla_{rad} < \nabla_s, \nabla_L \text{ for stability}$$

*The two conditions are equivalent for constant composition, but otherwise Ledoux convection is more difficult.*

## Caveat:

$$\nabla_L = \nabla_s + \frac{\beta}{4-3\beta} \nabla_\mu$$

This is an approximation that is valid only for a mixture of ideal gas and radiation pressure. The general relation is more complicated if the gas is degenerate or includes pairs.

See Kippenhahn and Weigert and Heger, Woosley, and Spruit (ApJ, 626, 350 (2005) Appendix A) for a general treatment and for what is implemented in Kepler.

*Semiconvection* is the term applied to the slow mixing that goes on in a region that is stable by the strict Ledoux criterion but unstable by the Schwarzschild criterion.

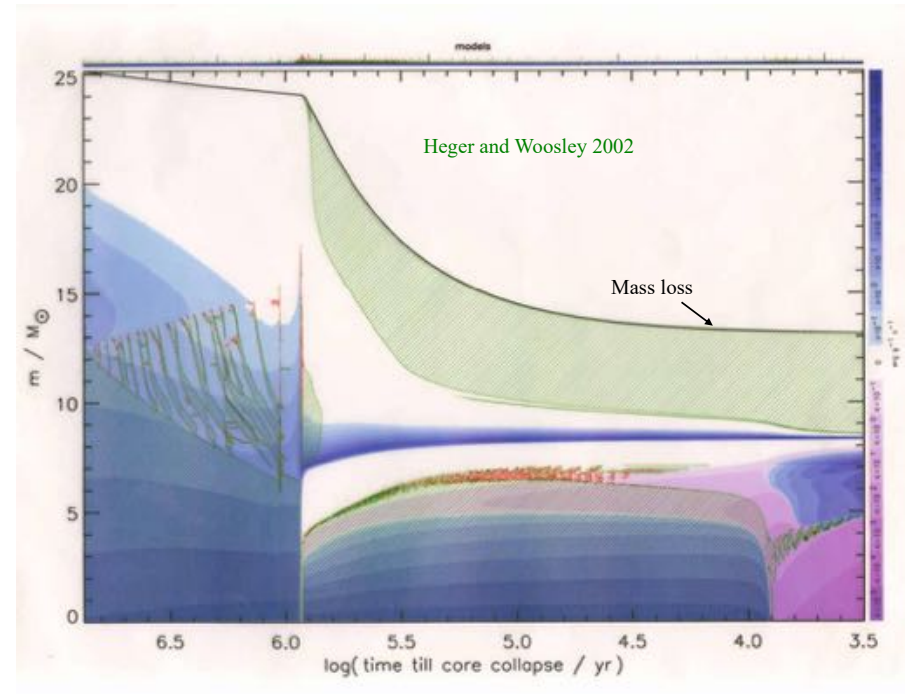
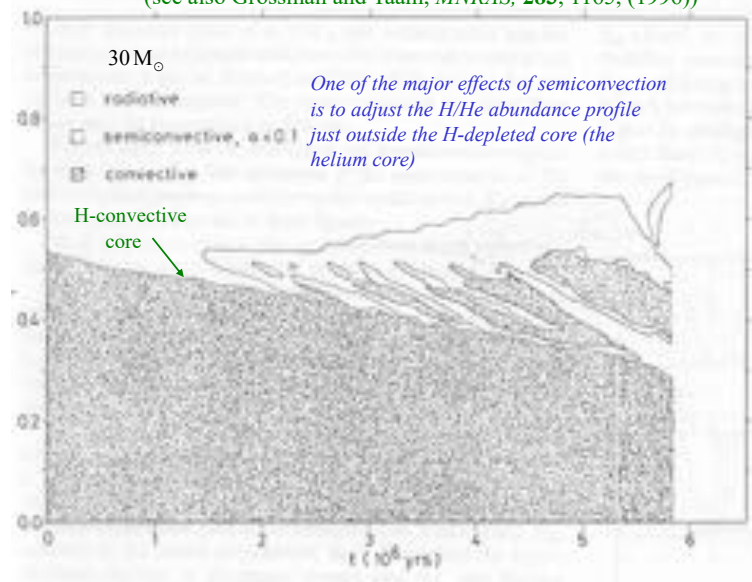
Generally it is thought that this process does not contribute appreciably to energy transport (which is then by radiative diffusion in semiconvective zones), but it does slowly mix the composition. Its efficiency can be measured by a diffusion coefficient that determines how rapidly this mixing occurs.

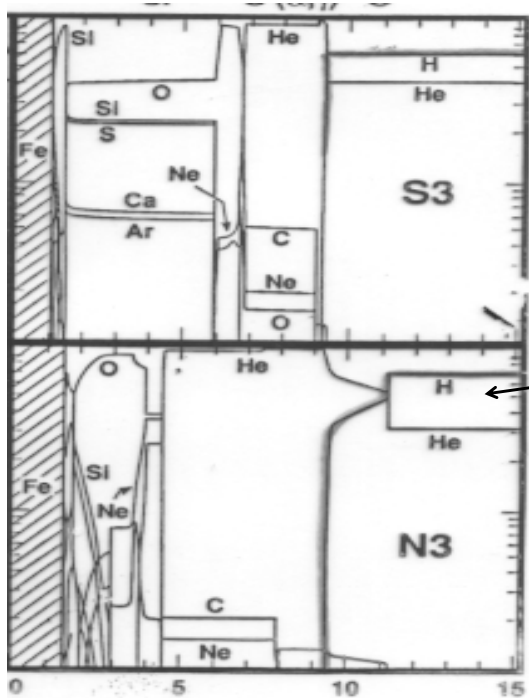
Many papers have been written both regarding the effects of semiconvection on stellar evolution and the estimation of this diffusion coefficient.

There are three places it is known to have potentially large effects:

- Following hydrogen burning just outside the helium core
- During helium burning to determine the size of the C-O core
- During silicon burning

Langer, El Eid, and Fricke, *A&A*, **145**, 179, (1985)  
(see also Grossman and Taam, *MNRAS*, **283**, 1165, (1996))





Woosley and Weaver (1990)

$$D_{semi} \sim 0.1 D_{rad}$$

surface convection zone

$$D_{semi} \sim 10^{-4} D_{rad}$$

- Shallower convection in H envelope
- Smaller CO core

For Langer et al.,  $\alpha \sim 0.1$  (their favored value) corresponds to  $D_{semi} \sim 10^{-3} D_{rad}$ , though there is not a real linear proportionality in their theory. The default in Kepler is  $D_{semi} = 0.1 D_{rad}$ .

By affecting the hydrogen abundance just outside the helium core, which in turn affects energy generation from hydrogen shell burning and the location of the associated entropy jump, semiconvection affects the envelope structure (red or blue) during helium burning. The two solutions are very narrowly separated and giant stars often spend appreciable time as both.

**Pure Ledoux mixing gives many more red supergiants.** Too many.

A critical test is predicting the observed ratio of blue supergiants to red supergiants. This ratio is observed to increase rapidly with metallicity (the LMC and SMC have a smaller proportion of BSGs than the solar neighborhood).

Semiconvection alone, without rotational mixing, appears unable to explain both the absolute value of the ratio and its variation with  $Z$  (Langer & Maeder, *A&A*, **295**, 685, (1995)). Ledoux gives answer at low  $Z$  but fails at high  $Z$ . Something in between L and S favored overall, with rotational mixing included as well.

*More semi-convection implies more BSG's*  
*Less semi-convection implies more RSG's*

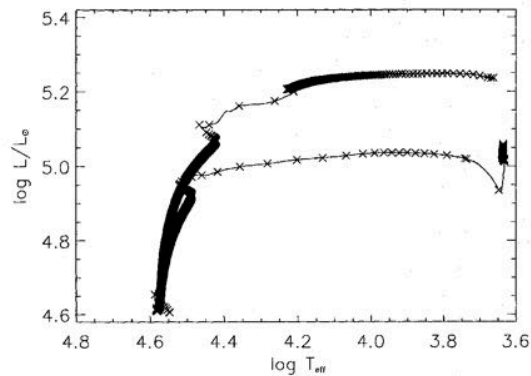


**Fig. 3.** Evolutionary tracks in the HR diagram for two  $20 M_{\odot}$  stars. The lower track is computed with semiconvection (cf. Fig. 1, and seq. # 2 in Table 2), the upper track with the Schwarzschild criterion for convection and with convective core overshooting (seq. # 5). The distance in time between two successive crosses on the tracks is 5000 yr

Langer and Maeder (1995)

**Table 1.** The B/R ratio in galaxies. Unless specified B means O, B and A stars

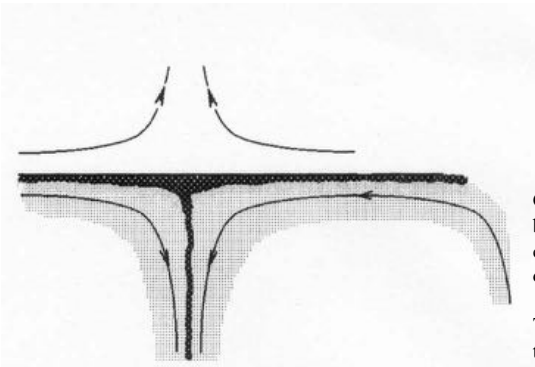
SN = solar neighborhood

Z	SMC	LMC	outer MW	SN	inner MW
Stars, $M_{hel} < -7^m 5^{\dagger}$	4	10	14	28	48:
Associations, $M_{hel} < -7^m 5^{\dagger}$	4	10	14	30	89:
Clusters, $M_V < -2^m 5^{\ddagger}$	2.5	6.7	7.7		20
counting only B supergiants					
NGC 330	0.5 ... 0.8				
Young clusters				3.6	

<sup>†</sup> Humphreys & McElroy (1984)

<sup>‡</sup> Meylan & Maeder (1982)

*Using Schwarzschild works for the galaxy but predicts B/R should increase at lower Z (weaker H shell), in contradiction with observations. Ledoux gives the low metallicity values OK but predicts too few BSG for the higher metallicity regions.*



Spruit (1992)

Convective cells form bounded by thin layers where the composition change is expressed almost discontinuously.

The diffusion coefficient is approximately the harmonic mean of the radiative diffusion coefficient and a much smaller ionic diffusion coefficient

Fig. 2. Thermal (light shading) and solute (heavy shading) boundary layers at a diffusive interface. The solute boundary layer is much thinner than the thermal boundary layer due to the lower diffusivity. Descending and ascending plumes carry heat and solute away from the interface

$$\kappa_{s, \text{eff}} = (\kappa_s \kappa_t)^{1/2} \left( \frac{4}{\beta} - 3 \right) \frac{\nabla_r - \nabla_a}{\nabla_\mu} \min \left[ 1, \frac{1}{2} q^{3/2} \right]$$

q is a correction factor that applies when the convective turnover is short relative to the diffusion time. Spruit argues that q typically < 1.

Moore and Garaud *ApJ*, **817**, 54, (2016)

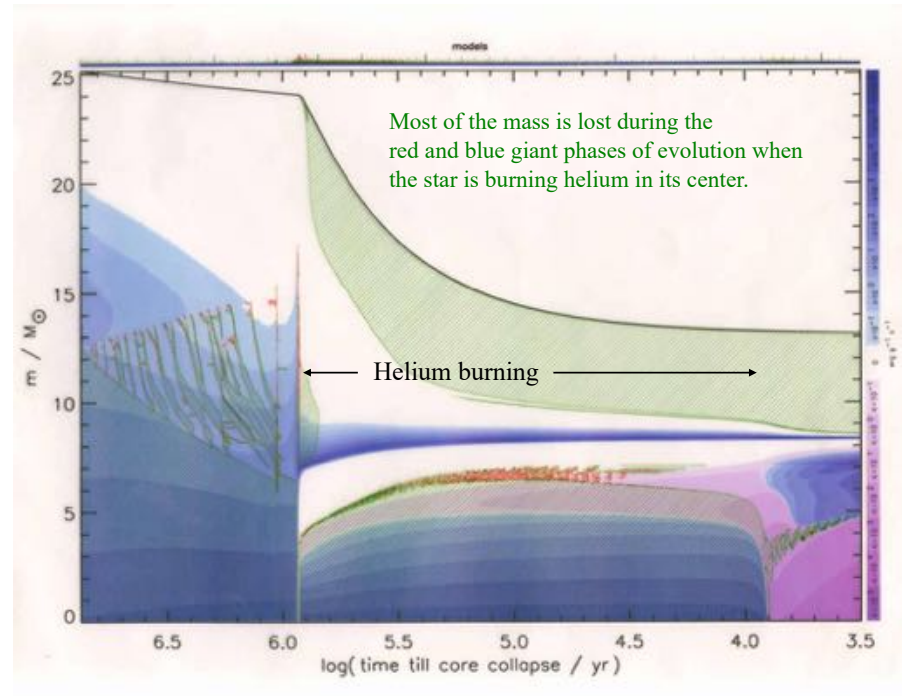
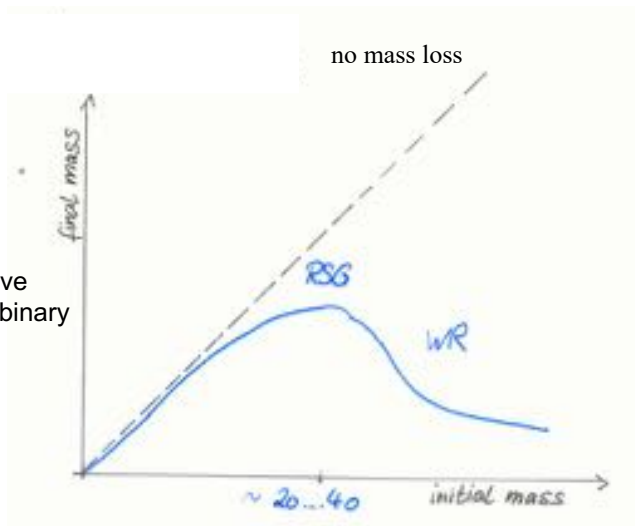
Study layer formation and break down in main sequence stars from 1.2 to 1.7 solar masses and conclude the layers are rapidly eroded and thus that Schwarzschild convection is essentially the right answer. **Semiconvection is very efficient.**

Problem still not explored for massive stars and advanced burning stages.

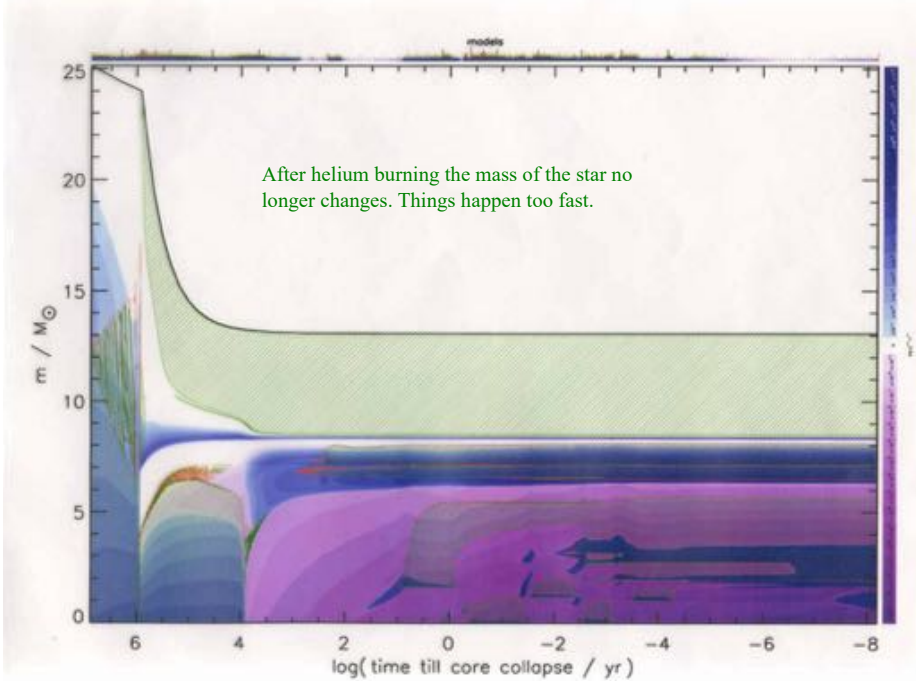
Probably Ledoux plus strong semiconvection favored for now, but overshoot and rotation can have similar effects. Still work to be done on a coherent general solution.

## Mass Loss

Maximum final mass is Z-sensitive and changed by binary mass exchange.



Mass Loss – Implications in Massive Stars



- 1) May reveal interior abundances as surface is peeled off of the star. E.g., CN processing, s-process, He, etc.
- 2) Determines the final presupernova mass given the main sequence mass. Gives the FMF from the IMF
- 3) Structurally, the helium and heavy element core – once its mass has been determined is not terribly sensitive to the presence of a RSG envelope. If the entire envelope is lost however, the star enters a phase of rapid Wolf-Rayet mass loss that does greatly affect everything – the explosion, light curve, nucleosynthesis and remnant properties.
- 4) Mass loss sets an upper bound to the luminosity of red supergiants. This limit is metallicity dependent. For solar metallicity, the maximum mass star that dies with a hydrogen envelope attached is about 35 solar masses.

**Humphreys-Davidson Limit**

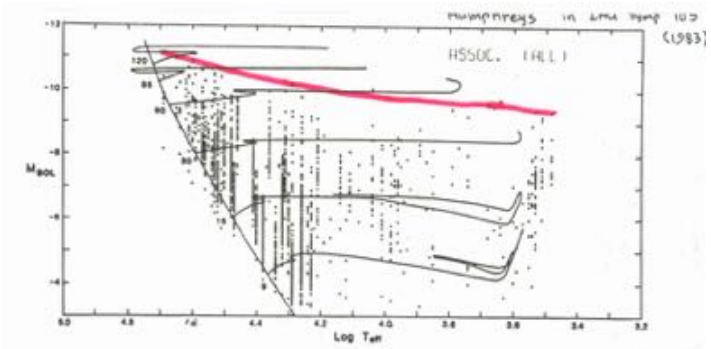


Figure 1 - The HR diagram,  $M_{sol}$  vs.  $\log T_{eff}$ , for O-type stars, supergiants, and less luminous early-type stars in 91 stellar associations and clusters in the solar region of our Galaxy.

Humphreys, R. M., & Davidson, K. 1979, ApJ, 232, 40  
 No RSG's brighter than  $M = -9$ .

- 5) Determines the lightest star that can become a supernova (and the heaviest white dwarf). Electron capture SNe? SNe I.5?
- 6) The nucleosynthesis ejected in the winds of stars can be important – especially WR-star winds.
- 7) In order to make gamma-ray bursts, the hydrogen envelope must be lost, but the Wolf-Rayet wind must be mild to preserve angular momentum.

## LBV's

Luminous blue variable stars lie to the left of the HD limit for very massive stars. Like BSG's but variable

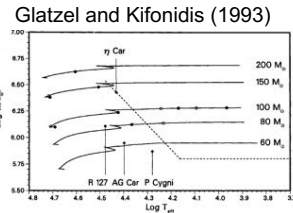
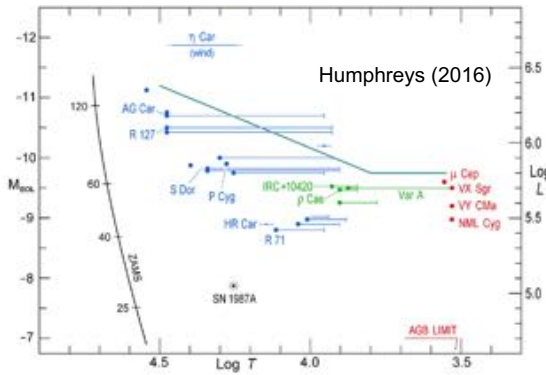


**Figure 4.** A schematic HR Diagram. A sample of known LBV/S Dor variables are shown in blue. The straight blue lines illustrate their apparent transits in the HRD during the LBV optically dense wind state. The dark green line is the upper luminosity boundary. Several cool (red) and warm hypergiants (green) are also shown.

"There is no consensus on the origin of the LBV instability, but most explanations invoke their proximity to their Eddington limit, and include the opacity-modified Eddington limit, rotation, super-Eddington winds, gravity-mode instabilities." Humphreys (2016)

For other stars – not hot or Wolf-Rayet – but especially for supergiants where most of the mass loss occurs use Nieuwenhuijzen and de Jager, *A&A*, **231**, 134, (1990)

$$\dot{M} = 9.63 \times 10^{-15} \left( \frac{L}{L_{\odot}} \right)^{1.42} \left( \frac{M}{M_{\odot}} \right)^{0.16} \left( \frac{R}{R_{\odot}} \right)^{0.81} M_{\odot} \text{ yr}^{-1}$$

which is an empirical fit across the entire HR-diagram. This is also multiplied by a factor to account for the metallicity-dependence of mass loss, typically  $Z^{0.5}$  to  $Z^{0.7}$  but this is especially uncertain.

The mass loss rates for red giants are less certain and involve different physics than main sequence stars, including possibly grain formation, pulsation, and/or extension to very large radii ( $\sim 10^{14}$  cm).

Mass loss for main sequence stars (Vink et al (2001) : Z scaling Vink et al (2001) and Pols et al (2009) suggest  $Z^{0.7}$

Table 3. Predicted mass-loss rates for different metallicities

$\Gamma_e$	$\log L_*$ ( $L_{\odot}$ )	$M_*$ ( $M_{\odot}$ )	$v_{\infty}/v_{esc}$	$T_{eff}$ (kK)	$\log \dot{M} (M_{\odot} \text{ yr}^{-1})$								
					1/100 Z/Z <sub>⊙</sub>	1/30 Z/Z <sub>⊙</sub>	1/10 Z/Z <sub>⊙</sub>	1/3 Z/Z <sub>⊙</sub>	1 Z/Z <sub>⊙</sub>	3 Z/Z <sub>⊙</sub>	10 Z/Z <sub>⊙</sub>		
0.130	5.0	20	2.6	50	-	-	-7.48	-7.03	-6.68	-6.23	-	-	
				45	-	-	-7.56	-7.12	-6.63	-6.22	-	-	
				40	-	-	-7.68	-7.18	-6.68	-6.29	-	-	
				35	-	-	-7.56	-7.09	-6.76	-6.45	-	-	
				30	-	-7.98	-7.45	-7.19	-6.92	-6.60	-	-	
				2.0	50	-	-7.79	-7.25	-6.88	-6.46	-6.01	-	-
				45	-	-7.93	-7.35	-6.91	-6.47	-5.97	-	-	
				40	-	-8.16	-7.47	-7.01	-6.48	-6.05	-	-	
				35	-	-8.45	-7.31	-6.93	-6.59	-6.29	-	-	
				30	-	-7.74	-7.31	-7.08	-6.76	-6.38	-	-	
0.206	5.5	40	2.6	50	-	-	-7.71	-7.40	-7.12	-6.73	-6.26	-	
				25	-	-	-7.76	-7.42	-7.04	-6.48	-6.01	-	
				22.5	-	-	-7.75	-7.40	-6.84	-6.32	-5.99	-	
				20	-	-	-7.71	-7.24	-6.72	-6.41	-6.06	-	
				17.5	-	-	-7.66	-7.24	-6.88	-6.49	-6.12	-	
				15	-	-	-7.88	-7.42	-6.98	-6.62	-6.15	-	
				12.5	-	-	-8.10	-7.61	-7.27	-6.74	-6.13	-	
				1.3	22.5	-	-7.49	-6.96	-6.55	-6.15	-5.75	-	
				20	-	-	-7.43	-6.99	-6.53	-6.22	-5.83	-	
				17.5	-	-	-7.50	-7.06	-6.63	-6.28	-5.83	-	
15	-	-	-7.53	-7.22	-6.85	-6.39	-5.79	-					
12.5	-	-	-7.71	-7.41	-7.04	-6.32	-5.72	-					
0.206	5.5	40	2.6	50	-	-	-7.30	-6.91	-6.36	-5.97	-5.53		
				45	-	-	-7.30	-7.12	-6.41	-5.95	-5.45		
				40	-	-	-7.45	-6.74	-6.47	-5.95	-5.53		
				35	-	-	-7.74	-6.92	-6.37	-6.06	-5.77		
				30	-	-	-7.10	-6.80	-6.58	-6.25	-5.90		
				-	-	-	-	-	-	-	-		

The driving mechanism of the winds of massive early type stars is radiation pressure on numerous spectral lines (Castor, Abbott, and Klein 1975).

Model atmosphere, line list, Monte Carlo radiation transport

Except for the most massive stars mass loss on the main sequence is small.

KEPLER

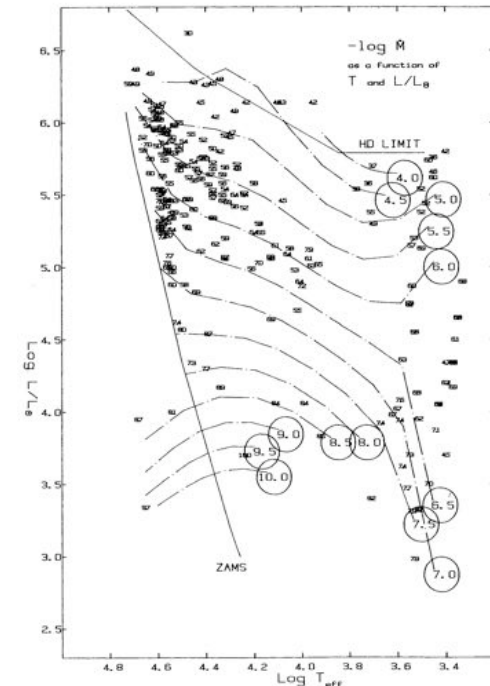
$\tau_{MS}(20 M_{\odot}) = 8 \text{ My}$   
 $T_{eff} = 30,000 \text{ K}$   
 $\Delta M < 1 M_{\odot}$   
 (19.55 not using Vink)  
 $\log(L/L_{\odot}) = 4.8$

de Jager, Nieuwenhuijzen, and van der Hucht (1988) *Aston, Ap. Suppl.*, **72**, 259

Circled numbers are  $-\log$  base 10 of the mass loss rate.

e.g.,  $30 M_{\odot}$   
 H-dep  $28.15 M_{\odot}$   
 He-dep  $12.80 M_{\odot}$   
 He-core  $10.80 M_{\odot}$

Solar metallicity stars over  $\sim 35 M_{\odot}$  lose their entire H envelope.



with mass loss, the final mass of a star does not increase monotonically with its initial mass. (e.g., Schaller et al. A&A, (1992)). These mass loss rates are now regarded as too large.

Initial Mass	Final Mass		
	Z=0.02 (Sch92)	Z=0.015 (Woo07)	Z=0.001 (Sch92)
7	6.8		6.98
9	8.6		8.96
12	11.5	10.9	11.92
15	13.6	12.8	14.85
20	16.5	15.9	19.4
25	15.6	15.8	24.5
40	8.12	15.3	38.3
60	7.83	7.29	46.8
85	8.98	6.37	61.8
120	7.62	6.00	81.1

He-core  
uncovered

Will be larger  
with current mass  
loss rates

*Because of the assumed dependence of mass loss on metallicity, stars of lower metallicity die with a higher mass. This has consequences for both the explosion and the nucleosynthesis.*

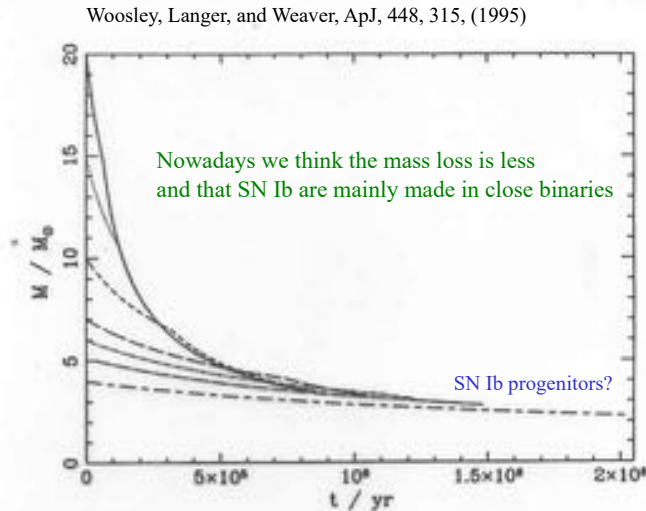


FIG. 1.—Total stellar mass as function of time for our sequences with initial masses of 20, 15, 10, 7, 6, 5, and 4  $M_{\odot}$ . Mass convergence due to mass-dependent mass loss is clearly visible.

### Wolf-Rayet stars – Langer, A&A, 220, 135, (1989)

$$\dot{M}_{WR} = (0.6-1.0) \times 10^{-7} \left( \frac{M_{WR}}{M_{\odot}} \right)^{2.5} M_{\odot} \text{ yr}^{-1}$$

Wellstein and Langer (1998) corrected this for Z-dependence and divided by 3 to correct for clumping.

$$\log(-\dot{M}_{WR} / M_{\odot} \text{ yr}^{-1}) = -11.95 + 1.5 \log(L / L_{\odot}) - 2.85 X_s$$

for  $\log(L / L_{\odot}) \geq 4.5$

$$= -35.8 + 6.8 \log(L / L_{\odot})$$

for  $\log(L / L_{\odot}) < 4.5$

Here  $X_s$  is the surface hydrogen mass fraction (WN stars) and the result should be multiplied by  $1/3 (Z/Z\text{-solar})^{1/2}$ .

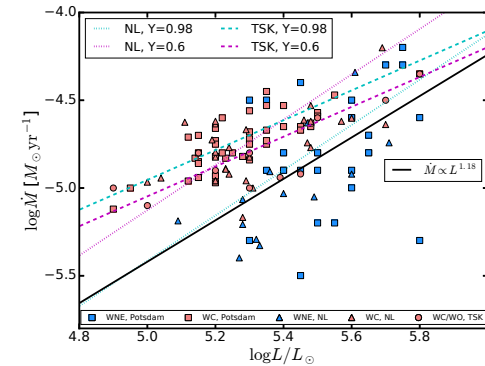


Figure 1. Empirical mass-loss rates of hydrogen-free WNE, WC, and WO stars in our galaxy, compared with the NL and TSK prescriptions (dotted and dashed lines). The Potsdam, NL and TSK samples are denoted by squares, triangles, and circles, respectively. WNE and WC/WO stars are marked by blue and coral colors, respectively. Here, a correction for a clumping factor of  $D = 10$  was applied to the mass-loss rates of the Potsdam WNE stars, to be consistent with the other empirical WR mass-loss rates (see the text). The thick black solid line gives the result of our new prescription for WNE stars, based on the Potsdam WNE sample (Eq. (3) with  $f_{WR} = 1.0$ ).

Yoon (2017) gives a useful summary of current mass loss rates for WR stars (though see also Vink (2017))

For WNE stars, with helium and nitrogen-rich surfaces use with  $Y = 1 - Z$  (the  $\log Y$  term is thus small)

$$\log(-\dot{M}_{NL} / M_{\odot} \text{ yr}^{-1}) = -11.0 + 1.29 \log(L / L_{\odot}) + 1.7 \log Y + 0.5 \log Z$$

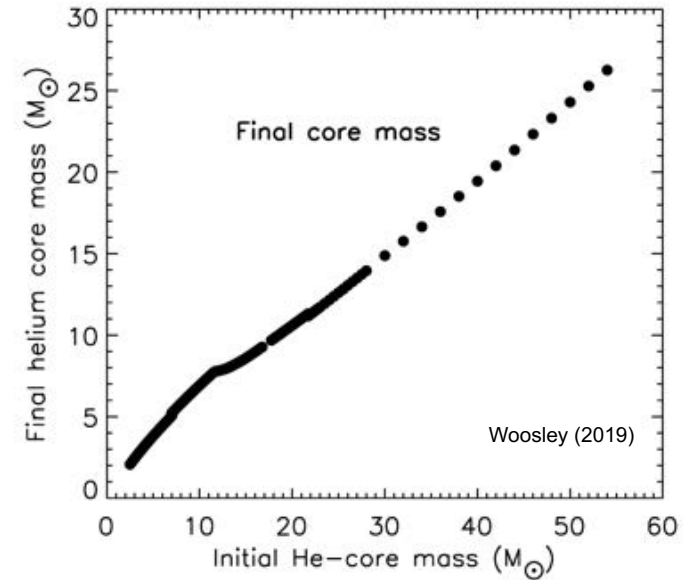
For WC and WO stars (stars with large C and O abundances at their surfaces) use (for  $Y < 0.9$ )

$$\log(-\dot{M}_{TSK} / M_{\odot} \text{ yr}^{-1}) = -9.20 + 0.85 \log(L / L_{\odot}) + 0.44 \log Y + 0.25 \log Z$$

In between  $Y = 1 - Z$  and .9, interpolate.

Using these formulae solar metallicity helium stars over  $10 M_{\odot}$  have a final mass equal to about half their initial mass at helium ignition (Woosley 2019)

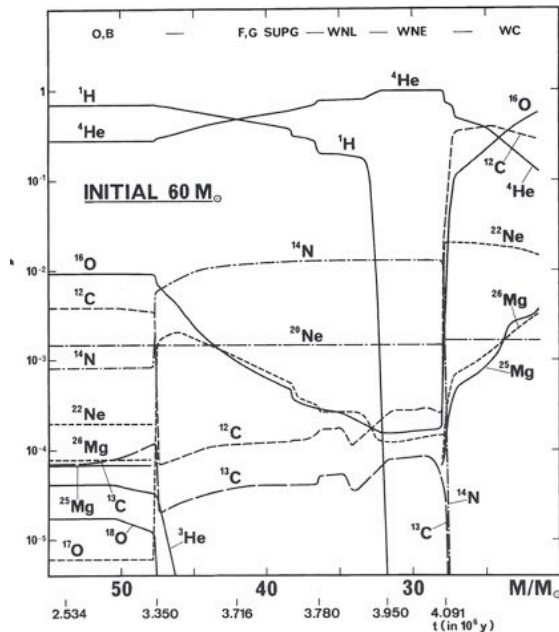
For helium stars



28

27 Massive Star Evolution with Mass Loss and Rotation

Maeder (1987)



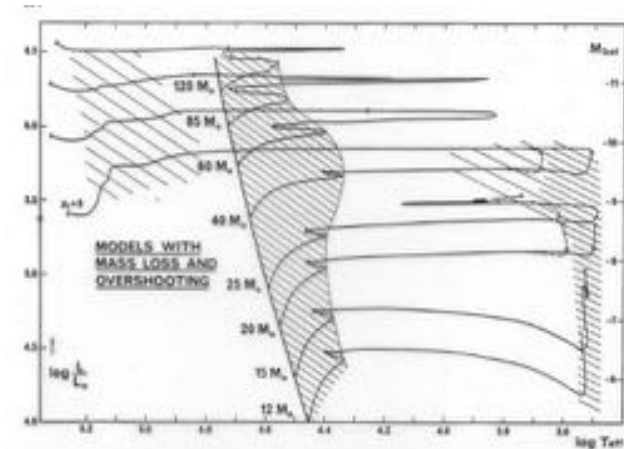
## CHARACTERISTICS OF WOLF RAYET STARS

- High luminosities ( $10^5 - 10^{6.5} L_{\odot}$ )
- Strong broad emission lines
- Dense optically thick winds
- High mass loss rates ( $\sim 10^{-5} - 10^{-4} M_{\odot} \text{ yr}^{-1}$ )
- High terminal wind speeds ( $1000 \text{ km s}^{-1}$ )
- Products of nucleosynthesis at surface especially He, N, C, O  
Hydrogen poor
- High surface temperature ( $30,000 - 100,000 \text{ K}$ )
- Wide range of masses; many are very massive  $8 - 25 M_{\odot}$   
and more (up to  $80 M_{\odot}$  for H-rich WR stars)

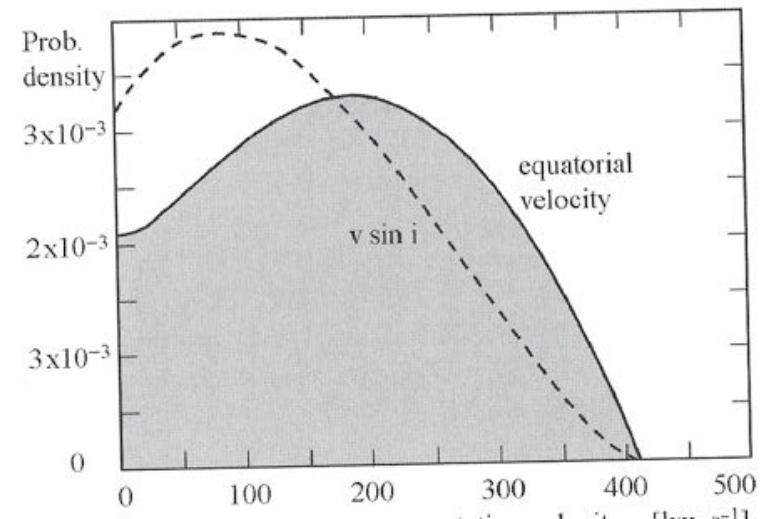
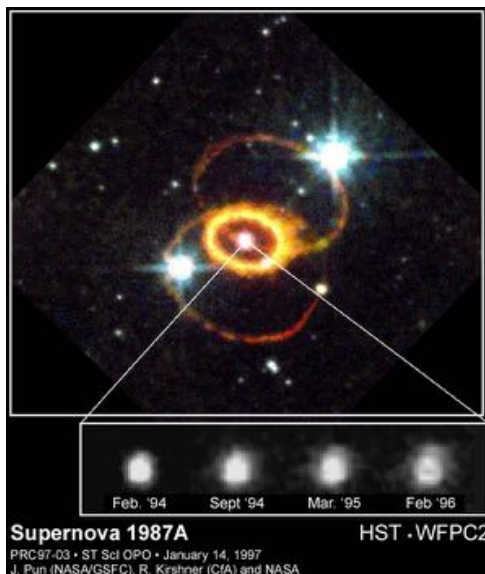
## Classification of Wolf-Rayet Stars

- "early" (hot; WxE) and "late" (cooler, WxL) types
- WN stars show helium lines (HeI, HeII) and lines of ionized nitrogen (NIII, NIV, NV)
- WC stars show lines of ionized carbon (CIII, CIV) and oxygen (OIV, OV, OVI)
- WC stars where oxygen lines dominate over carbon lines are also called WO stars.
- decreasing levels of ionization are denoted by decreasing arabic numbers
  - WNE = WN2...WN6
  - WNL = WN7...WN10
  - WCE = WC4...WC6
  - WCL = WC7...WC10
- WNE stars are subdivided in stars with strong (WNE-s) and weak (WNE-w) emission lines. WNE-s stars experience much higher mass loss rates than WNE-w stars. (Schmutz, Hamann, Wessolowski 1989, A&A, 210, 236)
- WNL stars show some (up to 40%) hydrogen

For single stars – Maeder and Meynet



## Rotation



Huang and Gies (2006) for 495 main sequence stars of Type B8 to O9.5. Analysis includes variation of line strength with effective gravity over surface of deformed rotating star. See also Huang et al (ApJ, 722, 605, (2010)). Many stars near rotational shedding limit.

## Eddington-Sweet Circulation

See Kippenhahn and Wiegert, Chapter 42, p 435ff for a discussion and mathematical derivation.

For a rotating star in which centrifugal forces are not negligible, the equipotentials where gravity, centrifugal force and pressure are balanced will no longer be spheres. A theorem, Von Zeipel's Theorem, shows that for a generalized potential

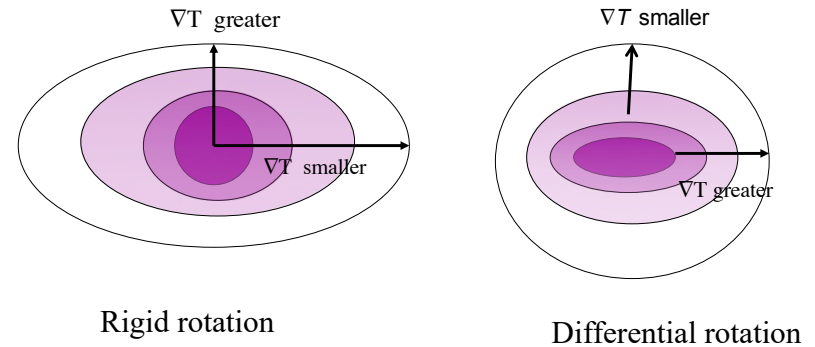
$$\Psi = \Phi + V = \text{gravitational potential} - \int_0^s \omega^2 s ds \quad \omega^2 s \vec{e}_s = -\nabla V$$

$$\nabla P = -\rho \nabla \Psi \quad \begin{array}{l} \text{generalization of} \\ \frac{dP}{dr} = -\frac{GM\rho}{r^2} \end{array} \quad \begin{array}{l} \text{centrifugal} \\ \text{potential} \end{array}$$

where  $s$  is the distance from the axis

Surfaces of constant  $\Psi$ , i.e., "equipotentials", will also be surfaces of constant pressure, temperature, density, and energy generation rate.

However, in this situation, the equipotentials will *not* be surfaces of constant heat flux because the temperature gradient normal to the surface will vary.



Rigid rotation

Differential rotation

As a consequence there will be regions that are heated relative to other regions at differing angles in the star resulting in some parts being buoyant compared with others. Thermal equilibrium is restored and hydrostatic equilibrium maintained if slow mixing occurs.

For rigid rotation and constant composition, the flows have the pattern shown on the following page.

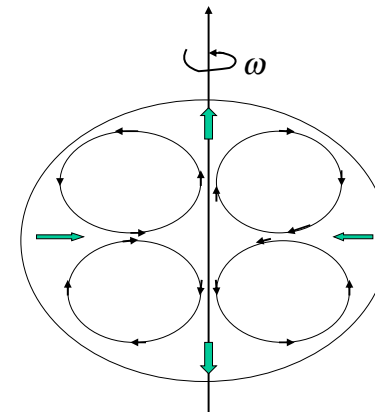
The time scale for the mixing is basically the time scale for the structure to respond to a thermal imbalance, i.e., the Kelvin Helmholtz time scale, decremented by a factor that is a measure of the importance of centrifugal force with respect to gravity.

$$\tau_{ES} \approx \frac{\tau_{KH}}{\chi} \quad \left( \frac{v_{rot}}{v_{esc}} \right)^2 = \frac{\omega^2 r^2}{2Gm} = \frac{3\omega^2}{8\pi G \bar{\rho}}$$

$$\tau_{KH} \approx \frac{GM^2}{RL} \quad \chi \approx \frac{\omega^2}{2\pi G \bar{\rho}} \sim \left( \frac{2\pi \tau_{ff}}{\tau_{rot}} \right)^2$$

→ 1 for rotational break up

## Eddington-Sweet Flow Patterns



Pattern for rigid rotation is outflow along the axes, inflow in the equator.

But this can be changed, or even reversed, in the case of differential rotation,

*Mixes composition and transports angular momentum (tends towards rigid rotation)*

For the sun,  $\tau_{KH} \approx 20 \text{ My}$ ,  $\bar{\rho} = 1.4 \text{ gm cm}^{-3}$ , and the rotational period is 28 days. So  $\omega \approx 3 \times 10^{-6} \text{ sec}^{-1}$ , so  $\chi \sim 10^{-5}$ , and the Eddington Sweet time scale is about  $10^{12}$  years, i.e., it is unimportant. It can become more important near the surface though as the density decreases (Kippenhahn 42.36)

*For a 20  $M_{\odot}$  star, the Kelvin Helmholtz time scale relative to the nuclear lifetime is about three times greater than in the sun. More importantly, because of rapid rotation,  $\chi$  is not so much less than 1. Eddington Sweet circulation is very important in massive stars where  $\tau_{KH}$  is still  $\ll \tau_{MS}$*

It is more complex however in the case of differential rotation and is inhibited by radially decreasing gradients in  $\bar{A}$ . *The latter makes its effect particularly uncertain, and also keeps the stars from completely mixing on the main sequence in the general case.*

*All instabilities will be modified by the presence of composition gradients*

- **Dynamical shear**

*sufficient energy in shear to power an overturn and do the necessary work against gravity*

- **Secular shear**

*same as dynamical shear but on a thermal time scale. Unstable if sufficient energy for overturn after heat transport into or out of radial perturbations. Usually a more relaxed criterion for instability.*

- **Goldreich-Schubert-Fricke**

*Axisymmetric perturbations will be unstable in a chemically*

*homogeneous region if  $\frac{dj}{dr} \leq 0$  or  $\frac{d\omega}{dz} \neq 0$*

- **Solberg Hoiland**

*Like a modified criterion for convection including rotational forces. Unstable if an adiabatically displaced element has a net force (gravity plus centrifugal force plus buoyancy) directed along the displacement*

$$\text{Stability if } \frac{g}{\rho} \left[ \left( \frac{d\rho}{dr} \right)_{ad} - \frac{d\rho}{dr} \right] + \frac{1}{r^3} \frac{d}{dr} (r^2 \omega)^2 \geq 0$$

Other instabilities that lead to mixing and the transport of angular momentum: See Heger et al, *ApJ*, **528**, 368 (2000) Collins, Structure of Distorted Stars, Chap 7.3,7.4; Maeder's text

energy available from shear adequate to (dynamically) overturn a layer. Must do work against gravity and any compositional barrier.

dynamical shear

secular shear

Goldreich-Schubert-Fricke instability

Eddington-Sweet circulation

Solberg-Høiland instability

(Endal & Sofia 1978, Pinsonneault, Kawaler, Sofia, Demarque 1989)

$$\frac{\partial j}{\partial r} > 0 \text{ for stability}$$

Eddington-Sweet and shear dominate.

Some historic calculations including angular momentum transport:

Kippenhan et al., *A&A*, **5**, 155, (1970)

Endal & Sofia, *ApJ*, **210**, 184, (1976) and **220**, 279 (1978)

*artificial rotation profiles and no transport (76) or large mu-barriers (78)*

Pinsonneault et al, *ApJ*, **38**, 424, (1989)

*the sun; improved estimates and formalism*

Maeder & Zahn, *A&A*, **334**, 1000 (1998)

*More realistic transport, H, He burning only*

Heger, Langer, & Woosley, *ApJ*, **528**, 368, (2000)

*First "realistic" treatment of advanced stages of evolution*

Maeder & Meynet, *A&A*, **373**, 555, (2001)

Heger, Woosley, and Spruit, *ApJ*, **626**, 350, (2005)

*First inclusion of magnetic torques in stellar model*

Surface abundances studied by:

Ekstrom et al, *A&A*, **537**, 146, (2012)

Meynet & Maeder, *A&A*, **361**, 101, (2000)

Heger & Langer, *ApJ*, **544**, 1016, (2000)

## Results:

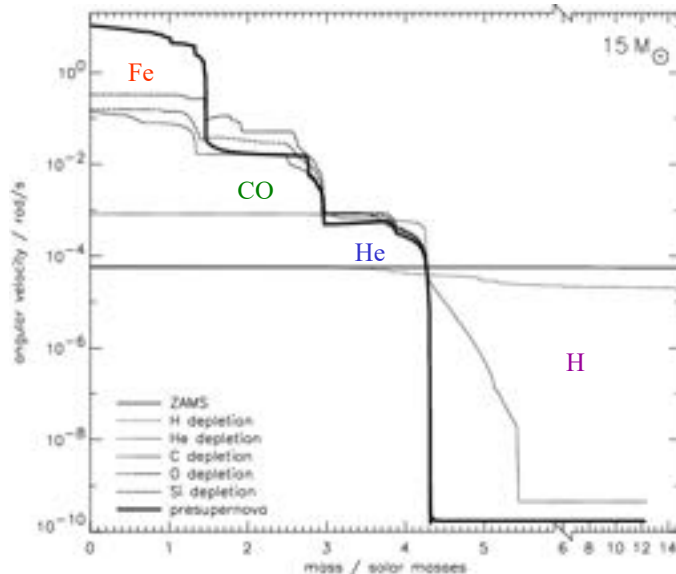
*In massive stars, Eddington Sweet dominates on the main sequence and keeps the whole star near rigid rotation. Later dynamical shear dominates in the interior.*

- Fragile elements like Li, Be, B destroyed to a greater extent when rotational mixing is included. More rotation, more destruction.
- Higher mass loss
- Initially luminosities are lower (because  $g$  is lower) in rotating models. later luminosity is higher because He-core is larger
- Broadening of the main sequence; longer main sequence lifetime
- More evidence of CN processing in rotating models. He,  $^{13}\text{C}$ ,  $^{14}\text{N}$ ,  $^{17}\text{O}$ ,  $^{23}\text{Na}$ , and  $^{26}\text{Al}$  are enhanced in rapidly rotating stars while  $^{12}\text{C}$ ,  $^{15}\text{N}$ ,  $^{16,18}\text{O}$ , and  $^{19}\text{F}$  are depleted.
- Decrease in minimum mass for WR star formation.

These predictions are in good accord with what is observed.

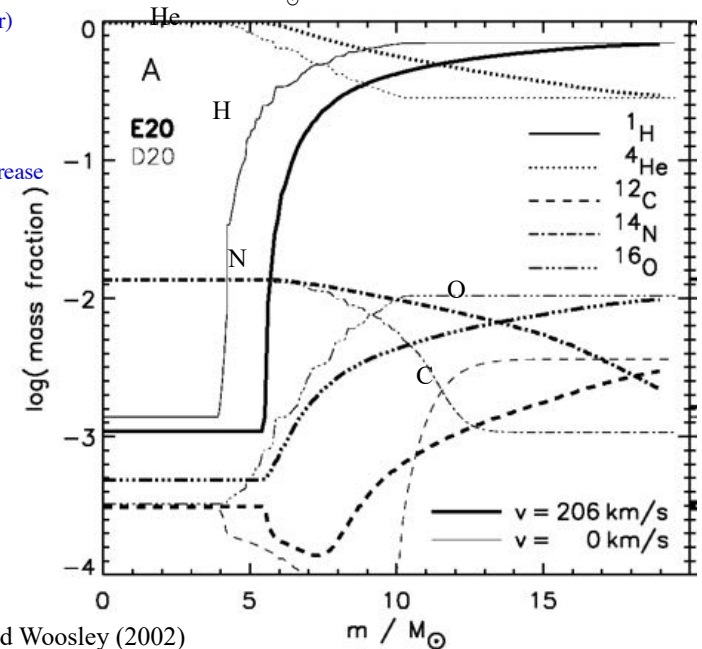
### Evolution Including Rotation

Heger, Langer, and Woosley (2000), *ApJ*, 528, 368



He  $\uparrow$  (He core larger)  
 C same but  $\downarrow$   
 N  $\uparrow$   
 O same but  $\downarrow$   
 Mass loss would increase the effects

### 20 $M_{\odot}$ Near Hydrogen Depletion



Heger, Langer, and Woosley (2002)

## B-fields

Final angular momentum distribution is important to:

- Determine the physics of core collapse and explosion
- Determine the rotation rate and magnetic field strength of pulsars
- Determine the viability of models for gamma-ray bursts.

The magnetic torques are also important for transporting angular momentum. The magnitude of the torque is approximately: Maeder - eq. 13-94  

$$S \sim \frac{B_r B_\phi}{4\pi} \quad \frac{dL}{dt} \sim S R^3$$
 with L the angular momentum  $S = \frac{1}{4\pi} \vec{r} \times (\vec{\nabla} \times \vec{B}) \times \vec{B}$

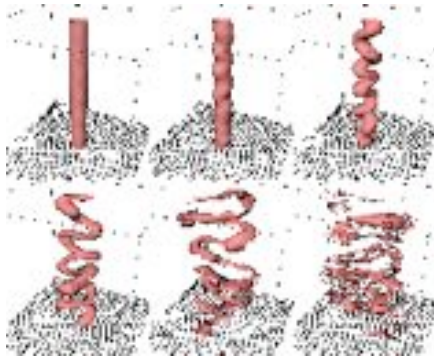
Spruit and Phinney, *Nature*, **393**, 139, (1998)

*Assumed  $B_r$  approximately equal  $B_\phi$  and that  $B_\phi$  was from differential winding. Got nearly stationary helium cores after red giant formation. Pulsars get rotation from "kicks".*

Spruit, *A&A*, **349**, 189, (1999) and **381**, 923, (2002)

$B_r$  given by currents from an interchange instability. Much smaller than  $B_\phi$ . Torques greatly reduced

Heger, Woosley, and Spruit, *ApJ*, **626**, 350, (2005); Woosley and Heger, *ApJ*, **637**, 914 (2006) ; Yoon and Langer, *A&A*, **443**, 643 (2006) implemented Spruit's formalism in stellar models.



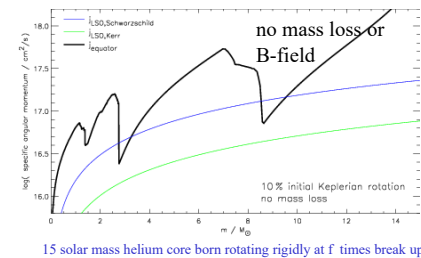
$$\text{Torque} \propto B_r B_\phi$$

$B_\phi$  from differential winding  
 $B_r$  from Taylor-Spruit dynamo

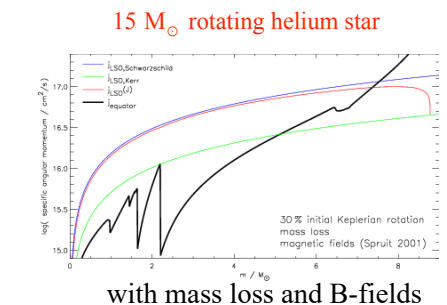
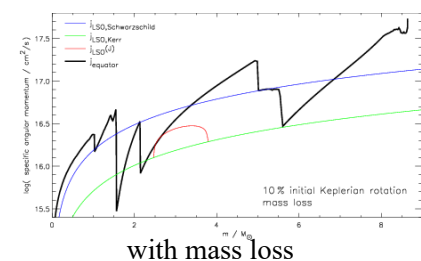
"Any purely poloidal field should be unstable to instabilities on the magnetic axis of the star" (Taylor 1973)

Spruit (2002, 2006)  
 Braithwaite (2006)  
 Denissenkov and Pinsonneault (2006)  
 Zahn, Brun, and Mathis (2007)

Approximately confirmed for white dwarf spins (Suijs et al 2008)



*If include WR mass loss and magnetic fields the answer is greatly altered....*



Stellar evolution including approximate magnetic torques gives slow rotation for common supernova progenitors. (solar metallicity)

Table 4: Pulsar Rotation Rate With Variable Remnant Mass<sup>a</sup>

Mass	Baryon <sup>b</sup> (M <sub>⊙</sub> )	Gravitational <sup>c</sup> (M <sub>⊙</sub> )	J (M <sub>bary</sub> ) (10 <sup>47</sup> erg s)	BE (10 <sup>53</sup> erg)	Period <sup>d</sup> (ms)
12 M <sub>⊙</sub>	1.38	1.26	5.2	2.3	15
15 M <sub>⊙</sub>	1.47	1.33	7.5	2.5	11
20 M <sub>⊙</sub>	1.71	1.52	14	3.4	7.0
25 M <sub>⊙</sub>	1.88	1.66	17	4.1	6.3
35 M <sub>⊙</sub> <sup>e</sup>	2.30	1.97	41	6.0	3.0

<sup>a</sup> Assuming a constant radius of 12 km and a moment of inertia 0.35MR<sup>2</sup> (Lattimer & Prakash 2001)

<sup>b</sup> Mass before collapse where specific entropy is 4 k<sub>B</sub>/baryon

<sup>c</sup> Mass corrected for neutrino losses

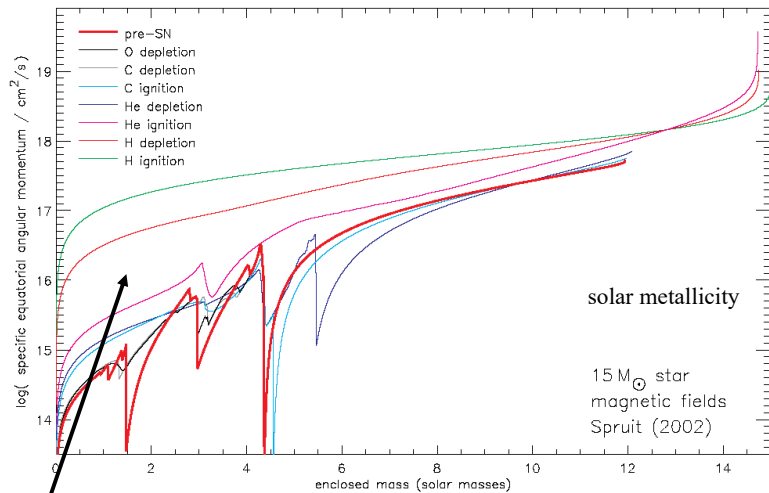
<sup>d</sup> Not corrected for angular momentum carried away by neutrinos

<sup>e</sup> Became a Wolf-Rayet star during helium burning

magnetar progenitor?

PreSN cores rotate more rapidly for more massive stars

Heger, Woosley, & Spruit (2004) using magnetic torques as derived in Spruit (2002)



Much of the spin down occurs as the star evolves from H depletion to He ignition, i.e. forming a red supergiant.

Heger, Woosley, & Spruit (2004)

This is consistent with what is estimated for young pulsars

Table 5: Periods and Angular Momentum Estimates for Observed Young Pulsars

pulsar	current (ms)	initial (ms)	J <sub>o</sub> (erg s)
PSR J0537-6910 (N157B, LMC)	16	~10	8.8 × 10 <sup>47</sup>
PSR B0531+21 (crab)	33	21	4.2 × 10 <sup>47</sup>
PSR B0540-69 (LMC)	50	39	2.3 × 10 <sup>47</sup>
PSR B1509-58	150	20	4.4 × 10 <sup>47</sup>

Implications:

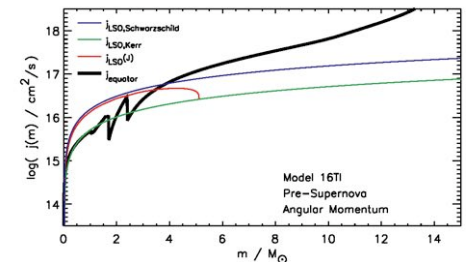
from HWS04

Rotation not dominant source of energy in common supernovae  
Gamma-ray bursts require special circumstances

## Chemically Homogeneous Evolution

- If rotationally induced chemical mixing during the main sequence occurs faster than the built-up of chemical gradients due to nuclear fusion the star evolves chemically homogeneous (Maeder, 1987)

$$\frac{\tau_{ES}}{\tau_{MS}} < 1$$



Woosley and Heger (2006)

- The star evolves blueward and becomes directly a Wolf Rayet (no RSG phase). This is because the envelope and the core are mixed by the meridional circulation -> **no Hydrogen envelope**
- Because the star is not experiencing the RSG phase it retains a **higher angular momentum in the core** (Woosley and Heger 2006; Yoon & Langer, 2006)

